VISCOUS FLOW STRUCTURE INTERACTION

by

Antonio Huerta, Graduate Student

and

Wing Kam Liu, Member, ASME

Department of Mechanical Engineering
Northwestern University
Evanston, Illinois 60201

To be presented at the "Symposium on Analysis and Testing of Vibrational and Seismic Response of Fluid-Structure Systems," 1987 ASME PVP Conference to be held in San Diego, California, June 28 to July 2, 1987.

Abstract

Considerable research activities in vibration and seismic analysis for various fluid-structure systems have been carried out in the past two decades. Most of the approaches are formulated within the framework of finite elements, and the majority of work deals with inviscid fluids. However, there has been little work done in the area of fluid-structure interaction problems accounting for flow separation and nonlinear phenomenon of steady streaming. In this paper, the Arbitrary Lagrangian Eulerian (ALE) finite element method is extended to address the flow separation and nonlinear phenomenon of steady streaming for arbitrarily shaped bodies undergoing large periodic motion in a viscous fluid. The results are designed to evaluate the fluid force acting on the body; thus, the coupled rigid body-viscous flow problem can be simplified to a standard structural problem using the concept of added mass and added damping. Formulas for these two constants are given for the particular case of a cylinder immersed in an infinite viscous fluid. The finite element modeling is based on a pressure-velocity mixed formulation and a streamline upwind Petrov/Galerkin technique. All computations are performed using a personal computer.

1. Introduction

This paper describes the application of the Arbitrary Lagrangian Eulerian (ALE) viscous fluid formulation [1] to evaluate the fluid force acting on a vibrating rigid body. The motion of an oscillating body is governed by its mass, the stiffness of the spring, the damping coefficient, the surrounding viscous fluid and the external force acting on the solid (see Figure 1). In current engineering practice, the influence of an inviscid fluid is taken into account by means of a hydrodynamic mass or an added mass [2,3]. When dealing with viscous fluids, the added mass cannot describe properly the force acting on the body, thus, an added damping term is needed. To avoid coupling between the spring-mass system and the nonlinear Navier-Stokes equations, the equation of motion for the rigid body is simplified to:

$$M\ddot{d} + C\dot{d} + Kd = F_{ext} - F_f \tag{1}$$

where M, C, K, F_{ext} and d are the mass, structural damping coefficient, structural spring constant, external force, and displacement, respectively, of the rigid body. A superposed dot denotes material time differentation. F_f is the resultant fluid force acting on the body (i.e., without actually modeling the viscous fluid) and it is assumed of the form:

$$F_f = M_{ad}\ddot{d} + C_{ad}\dot{d} \tag{2}$$

where M_{ad} and C_{ad} are the added mass and added damping coefficients, respectively. Substituting Eq. (2) into Eq. (1) yields

$$(M + M_{ad})\ddot{d} + (C + C_{ad})\dot{d} + Kd = F_{ext} \tag{3}$$

which can be solved readily since it is a standard one degree of freedom structural dynamic equation, provided M_{ad} and C_{ad} are evaluated properly. M_{ad} and C_{ad} can be estimated by prescribing to the rigid body a sinusoidal motion

$$d = s_o \sin \omega t \tag{4}$$

where s_o, ω and t are the amplitude of the motion, circular frequency and

time, respectively.

In the next section, the governing equations for a viscous fluid subject to a large boundary motion, such as given by Eq. (4), are formulated. In Section 3, the computational procedures for M_{ad} and C_{ad} using the ALE method are described. An application to a circular cylinder oscillating in a viscous fluid is given in Section 4. The concluding remarks are presented in Section 5.

2. Governing Equations for Viscous Fluids in ALE Formulation

Consider a fluid domain R described by material, spatial, or referential coordinates which are denoted by $\underset{\sim}{X}$, $\underset{\sim}{x}$ and $\underset{\sim}{\chi}$, respectively. Throughout this paper, repeated indices denote a summation over the number of space dimensions (NSD). The spatial derivative (i.e., derivative with respect to $\underset{\sim}{x}$) is designated by a comma followed by a subscript while the material, spatial and referential time derivatives of an arbitrary function f are represented by $f_{,t[\underset{\sim}{X}]}$, $f_{,t[\underset{\sim}{x}]}$ and $f_{,t[\underset{\sim}{\chi}]}$, respectively. The continuity and Navier-Stokes equations for a Newtonian, isothermal fluid are [4,5]

$$\frac{1}{B} P_{,t[\underset{\sim}{X}]} + v_{i,i} = 0 \tag{5a}$$

and,

$$v_{i,t[\underset{\sim}{\chi}]} + c_j v_{i,j} = -\frac{1}{\rho} P_{,i} + \nu(v_{i,j} + v_{j,i})_{,j} + b_i \tag{5b}$$

where B is the bulk modulus of the fluid, P is the thermodynamic pressure; $\underset{\sim}{v}$ is the material velocity vector; ρ is the fluid density; ν is the kinematic viscosity; $\underset{\sim}{b}$ is the body force vector; and $\underset{\sim}{c}$ is the convective velocity vector. The convective velocity is defined as

$$c_i = v_i - \hat{v}_i \tag{6}$$

where $\underset{\sim}{\hat{v}}$ is the mesh velocity vector which is arbitrarily chosen depending on the particular problem [6,7].

The variational equations associated with Eqs. (5) are [7,8]

$$\int_{R_x} \delta P \frac{1}{B} P_{,t[\underset{\sim}{X}]} \, dR_x + \int_{R_x} \delta P \, v_{i,i} \, dR_x = 0 \tag{7a}$$

and,

$$\int_{R_x} \delta\tilde{v}_i \, v_{i,t[\chi]} \, dR_x + \int_{R_x} \delta\tilde{v}_i \, c_j \, v_{i,j} \, dR_x - \int_{R_x} \frac{1}{\rho} (\delta v_i)_{,i} \, P \, dR_x +$$

$$\int_{R_x} \frac{\nu}{2}[(\delta v_i)_{,j} + (\delta v_j)_{,i}][v_{i,j} + v_{j,i}] dR_x - \int_{R_x} \delta\tilde{v}_i b_i \, dR_x - \int_{\partial R_x^h} \delta v_i h_i \, dS = 0 \tag{7b}$$

The weighting function δP in (7a) is chosen to be discontinuous across the interelement boundaries and constant inside the element. The same function δP is used for the pressure interpolation completing a Galerkin formulation. On the other hand, the weighting function $\delta\tilde{v}_i$ in (7b) is composed of two terms: the first one, δv_i, is continuous within the elements and across their boundaries; and the second term is the discontinuous streamline contribution. In Eq. (7b) a Petrov/Galerkin formulation is used because the interpolation functions for the velocities are linear combinations of the continuous term, δv_i. Hughes and Brooks [9] present a detailed discussion on the assumptions required for obtaining Eq. (7b). It should be noted that the continuous part of the velocity weighting function, δv_i, must satisfy $\delta v_i = 0$ on the boundary where the velocity field is prescribed. The Cauchy stress traction, $\underset{\sim}{h}$, is applied to the rest of the fluid boundary.

The spatial discretization of Eqs. (7) via finite elements leads to the following two systems of matrix equations:

$$\underset{\sim}{M}^P \dot{\underset{\sim}{P}} + \underset{\sim}{G}^T \underset{\sim}{v} = \underset{\sim}{0} \tag{8a}$$

$$\underset{\sim}{M} \, \underset{\sim}{a} + \underset{\sim}{n}(\underset{\sim}{v}) + \underset{\sim}{K}_{\mu} \underset{\sim}{v} - \underset{\sim}{G} \, \underset{\sim}{P} = \underset{\sim}{f}^{ext} \tag{8b}$$

where $\underset{\sim}{M}^P$ is the pressure-mass matrix; $\underset{\sim}{M}$ is the fluid mass matrix; and $\underset{\sim}{v}$ and $\underset{\sim}{P}$ are the vectors of unknown nodal values for velocity and pressure, respectively. $\dot{\underset{\sim}{P}}$ is the material time derivative of $\underset{\sim}{P}$; $\underset{\sim}{a}$ is the time derivative of the material velocity vector, $\underset{\sim}{v}$, holding the reference fixed; (i.e., $\underset{\sim}{\chi}$ fixed), $\underset{\sim}{n}$ is the generalized convective velocity vector; $\underset{\sim}{f}^{ext}$ is the

total external load vector applied to the fluid, $\underset{\sim}{K}_{\mu}$ is the fluid viscosity matrix and $\underset{\sim}{G}$ is the divergence operator matrix.

Remark 1: If the fluid is assumed incompressible, Eqs. (8) are further simplified to

$$\underset{\sim}{G}^{T}\underset{\sim}{v} = \underset{\sim}{0} \tag{9a}$$

$$\underset{\sim}{M}\,\underset{\sim}{a} + \underset{\sim}{n}(\underset{\sim}{v}) + \underset{\sim}{K}_{\mu}\underset{\sim}{v} - \underset{\sim}{G}\,\underset{\sim}{P} = \underset{\sim}{f}^{ext} \tag{9b}$$

Remark 2: A predictor-multicorrector algorithm described in Refs. [1,10] is used to solve either Eqs. (8) or (9). Two passes (i.e., one iteration) are used to insure stability and account for the upwinding effects on the mass term.

In order to determine the dimensionless parameters governing the boundary value problem, the incompressible field equations (i.e., Eqs. (5)) are written in a nondimensional form [11]. The length scale used is the dimension b of the rigid body in the motion direction (see Fig. 1). The time scale is ω^{-1} and the characteristic velocity $v_o = s_o\omega$ is chosen to scale the velocities. Recall, from Eq. (4), that v_o is the amplitude of the prescribed velocity. Finally, $\mu v_o/b$ is the pressure scale where μ is the absolute viscosity of the fluid. In this analysis, the gravity is perpendicular to the plane under consideration (i.e., the body forces are zero) and incompressibility of the fluid is assumed. Consequently, scaling with b, ω^{-1} and v_o, Eqs. (5) become:

$$\bar{v}_{i,i} = 0 \tag{10a}$$

$$\bar{v}_{i,\bar{t}[\chi]} + \beta\,\bar{c}_j\bar{v}_{i,j} = \frac{1}{R_e}\left[\left[\bar{v}_{i,j} + \bar{v}_{j,i}\right]_{,j} - \bar{P}_{,i}\right] \tag{10b}$$

where the superscripted bars denote dimensionless functions, all the spatial

derivatives are with respect to dimensionless coordinates $\bar{x}_i = x_i/b$, β is an amplitude ratio parameter and R_w is the frequency Reynolds number. However, for inviscid fluids (i.e., R_w approaches to infinity) the right hand side of Eq. (10b) will become zero and the resulting equilibrium equations are not the classical Euler equations. Hence, a different pressure scaling is introduced. The characteristic pressure is defined as $\rho b\omega v_o$, and Eq. (10b) becomes

$$\bar{v}_{i,\bar{t}[\chi]} + \beta\, \bar{c}_j \bar{v}_{i,j} = \frac{1}{R_w}[\bar{v}_{i,j} + \bar{v}_{j,i}]_{,j} - \bar{P}_{,i} \qquad (10c)$$

The solution characteristics of this problem are governed by the two parameters in Eqs. (10) and α, which is associated with the geometry. They are defined as:

$$\alpha = \frac{D}{b} \quad , \quad \beta = \frac{s_o}{b} \quad , \quad \text{and } R_w = \frac{b^2\omega}{\nu} = \frac{Re}{\beta} \qquad (11)$$

where D is the diameter of the outer boundary of the fluid domain and Re is the Reynolds number (i.e., $Re = v_o b/\nu$). From Eq. (10b) one can notice that β and R_w are associated with convection and diffusion, respectively. Therefore, for "small" β and R_w the diffusion effects govern the velocity field; whereas, with "large" β and R_w the convection dominates.

In order to define the boundary value problem completely, the dimensionless boundary conditions and mesh velocities are given as follows. Velocity conditions need to be specified on the boundaries, whereas, the pressure needs to be fixed at one point in the fluid domain to obtain a pressure datum. On the outer cylinder and in the vertical direction along the symmetry line the fluid velocity is zero while on the rigid body the dimensionless form of the boundary condition, defined by Eq. (4), is given by:

$$\bar{v}_1(\bar{x}_{1i} + \bar{d}(\bar{t}), \bar{x}_{2i}) = \cos \bar{t} \tag{12a}$$

$$\bar{v}_2(\bar{x}_{1i} + \bar{d}(\bar{t}), \bar{x}_{2i}) = 0 \tag{12b}$$

where

$$\bar{d}(\bar{t}) = \beta \sin \bar{t} \tag{12c}$$

and $\bar{x}_i$ are the dimensionless coordinates for the contour of the inner body.

The influence of β on the equilibrium equation and on the motion of the inner boundary suggests that a perturbation technique can be used to solve this problem, see Ref. [11]. However, such a procedure is only valid for small β. Conversely, the Arbitrary Lagrangian Eulerian formulation used here does not restrain the magnitude of the amplitude ratio, β.

Unless a perturbation technique is used, the velocity conditions at the solid body boundary require a Lagrangian description. That is, the mesh must follow the particle movement at this boundary. However, elsewhere and principally away from the oscillating body, a Eulerian description is better suited because a fixed reference through which the fluid moves allows strong distortions due to the flow. Finally, in order to evaluate the boundary effect, the density of elements must increase in the vicinity of the moving solid. These requirements can be fulfilled by using an ALE formulation: (1) at the surface of the oscillating body the mesh motion is prescribed equal to the particle motion, (2) away from the solid the mesh is fixed and (3) in between, a transition zone is defined with an arbitrarily prescribed mesh motion. The mesh velocities can be defined as:

$$\hat{v}_1 = \begin{cases} \frac{s_o}{2}\left[1 + \cos\left(\frac{\ell\pi}{L}\right)\right]\omega \cos \omega t & \text{if } \ell \leq L \qquad (13a) \\ 0 & \text{if } \ell > L \qquad (13b) \end{cases}$$

and

$$\hat{v}_2 = 0 \qquad (13c)$$

where ℓ is the horizontal distance between the referential point (mesh node) and the rigid body surface, and L is an arbitrarily chosen transition length.

Finally it is noted that a streamline upwind Petrov/Galerkin formulation is required because of the relative importance of the convective effects. In general, the convective effect is increased in the vicinity of the moving solid. Therefore, for Reynolds numbers greater than 50, upwinding is necessary. A temporal, rather than spatial criterion [12], is selected for the perturbation of the weighting function because of the time dependency of $\underset{\sim}{c}$ and the increased convection which can occur in the smallest elements.

3. Determination of the Added Mass and Damping Coefficients

The evaluation of M_{ad} and C_{ad} is similar to the procedure described in Ref. [3]. That is, the body motion is prescribed and the fluid force, F_f, acting on the solid is evaluated. Since acceleration and velocity cannot be applied independently of each other (i.e., set the acceleration equal to one and the velocity to zero, or vice-versa) the prescribed sinusoidal motion defined by Eq. (4) is chosen. In this manner, F_f can be expanded using a Fourier series; and consequently, the term in phase with the acceleration is separated from the one in phase with the velocity. From these two terms, the added mass and damping can be computed. The Fourier decomposition of F_f is as follows:

$$F_f = A_o + \sum_{n=1}^{\infty} A_n \cos(n\omega t) + \sum_{n=1}^{\infty} B_n \sin(n\omega t) \tag{15}$$

where,

$$A_o = \frac{1}{2\pi} \int_o^{2\pi} F_f dt \quad , \tag{16a}$$

$$A_n = \frac{1}{\pi} \int_o^{2\pi} F_f \cos(n\omega t) dt \quad , \quad n = 1, \ldots \infty \tag{16b}$$

$$B_n = \frac{1}{\pi} \int_o^{2\pi} F_f \sin(n\omega t) dt \quad , \quad n = 1, \ldots \infty \tag{16c}$$

If the initial assumption that F_f is a linear combination of acceleration and velocity is true, only two coefficients (A_1 and B_1) are nonzero. Obviously, these coefficients are the ones associated with the same frequencies as the prescribed acceleration and velocity. Once A_1 and B_1 are computed from Eqs. (16b) and (16c), the added mass and damping are determined by

$$M_{ad} = -\frac{B_1}{s_o\omega^2} \tag{17a}$$

and

$$C_{ad} = \frac{A_1}{s_o\omega} \tag{17b}$$

respectively. Or, in dimensionless form, using the scaling factors defined in the previous section:

$$\overline{M}_{ad} = -\frac{B_1}{s_o\omega^2}\frac{1}{\rho b^2} \tag{18a}$$

and

$$\overline{C}_{ad} = \frac{A_1}{s_o\omega^2}\frac{1}{\rho b^2\omega} \tag{18b}$$

With reference to Fig. 1, the computation of F_f at every instant can be obtained by integrating both the thermodynamic pressure P and the viscous shear forces around the body. The added mass and damping parameters can then be computed; and the rigid body-viscous flow interaction problem is simplified to Eq. (3).

4. Numerical Examples

Numerical results are obtained for a circular body oscillating with a sinusoidal motion. The circular body shape is chosen in order to compare the hydrodynamic force obtained using this method with the Fritz formulas [2]. The latter is valid only for a cylinder immersed in inviscid fluids. The method described in this paper can account for an arbitrary geometry in a viscous fluid.

All calculations are performed in single precision (32 bits per word) on a 640 kilobyte IBM-XT personal computer with an 8087 mathematical processor.

The dimensionless parameter α is set to 30 throughout this analysis. The influence of the other two parameters governing the problem, namely β and R_w, is assessed by varying them in the following fashion: the amplitude ratio parameter, β, is taken equal to 0.1, 0.4, 0.75 and 1.0; the frequency Reynolds number, R_w, varies from 20 to infinity. In fact, these different cases represent a Reynolds number ($Re = R_w\beta$) which ranges between 2 and infinity.

The dimensionless time-step used in the computation is usually given by $\omega\Delta t = \frac{\pi}{20}$; however, in the cases highly dominated by diffusion or convection it is reduced to $\frac{\pi}{28}$. As shown in Fig. 2; the 224-node mesh consists of 195 4-node elements (constant pressure elements). Finally, the transition length for the mesh movement does not influence the results if $L > 9s_o$.

Figures 3 and 4 show the instantaneous streamlines for $\beta = 0.1$ and two frequency Reynolds numbers: 20 and 500. As expected, for high R_w most of shearing occurs in a small layer surrounding the rigid body. At $t = \frac{\pi}{2}$ a vortex clearly appears, but it disappears almost instantaneously. However, for large β and R_w the vortex does not disappear and vortex shedding occurs, see Fig. 5 where $\beta = 1.0$ and $R_w = 1000$. Although the purpose of this study is to compute the fluid force on the solid, Fig. 5 clearly suggests that a vortex

shedding analysis can be conducted with the present method if a finer mesh is used away from the solid boundary in order to capture the vortex movement.

The pressure distribution around the rigid body for $\beta = 0.1$ and $R_w = 20$ and 500 (i.e., Re = 2 and 50, respectively) is presented in Fig. 6. One can observe that the angle θ for the stagnation point decreases (i.e., tending to $\frac{\pi}{2}$) as R_w is increased at $t = 0$, and that the pressure amplitude decreases as R_w increases. The last phenomenon is also observed in Fig. 7, where the variation of the fluid reaction (F_f), is plotted versus time. The relative importance of the added mass and damping via the decomposition of F_f is also depicted in Fig. 7. For instance, the ratio of damping to mass force decreases from 75% at $R_w = 20$ to 15% at $R_w = 1000$.

It is important to notice that both added mass and damping are frequency dependent for viscous fluids. Figures 8 and 9 show the variations of the two parameters with R_w. From these figures, it can be concluded that added mass is independent of the amplitude ratio β, while the added damping varies with β. As expected, for all β, the added damping goes to zero and the added mass remains constant as R_w goes to infinity. The computed added mass for $R_w = \infty$ is 0.8169 which compares well (3.8% relative error) with Fritz's approximation (0.7871), given the coarseness of the mesh. If the added mass results are interpolated using Fritz formulas for the limit, the following equation is obtained:

$$\bar{M}_{ad} = 5.992\ R_w^{-0.643} + 0.787 \qquad (19)$$

with a correlation of 98.3%. Obviously, this correlation would be improved if the actual computed mass for $R_w = \infty$ was taken; however, Fritz formulas are the simplest and most extended way to approximate the value of the added mass for an inviscid fluid. The added damping interpolation is a little more complicated because the added viscosity is a function of β. However, Fig. 9

suggests that β only influences the slope of the Log-Log curve. Hence, the following interpolation is obtained:

$$\overline{C}_{ad} = 1.88\ (R_w/9.42)^{0.361\beta-0.618} \qquad (20)$$

and the curves plotted in Fig. 9 are derived from the direct application of Eq. (20) for different parameters β and R_w.

5. Conclusions

This paper shows that Arbitrary Lagrangian Eulerian techniques are applicable to vibration and seismic analysis for fluid-structure systems. An ALE formulation is presented for a viscous fluid subject to a large boundary motion. Because of the use of a pressure-velocity mixed formulation, and the improvements in accuracy of the streamline upwind Petrov/Galerkin techniques, the computer program is implemented on a personal computer.

The concept of added mass and damping is used to simplify the rigid body-viscous flow interaction problem into a standard structural dynamic analysis. When the fluid force on the solid is expanded via Fourier analysis, only the added mass and damping terms are nonzero. The hydrodynamic mass computed for the inviscid case agrees well with the Fritz formula.

A parametric analysis shows that M_{ad} is only a function of the frequency Reynolds number, and a simple formula is presented for the particular geometry studied here. On the other hand, the added damping depends on the frequency Reynolds number and the amplitude ratio of the motion. A simple formula is also obtained for the prediction of C_{ad} in this particular problem.

Acknowledgements

The financial assistance provided to Antonio Huerta by a Catalan Fellowship (CIRIT BE84-26) is gratefully acknowledged. The support of Wing K. Liu by the National Science Foundation is also gratefully acknowledged.

References

1. Liu, W. K. and Gvildys, J., "Fluid-Structure Interaction of Tanks with an Eccentric Core Barrel," Computer Methods in Applied Mechanics and Engineering, Vol. 58, pp. 51-57, 1986.

2. Fritz, R. J., "The Effect of Liquids on Dynamic Motions of Immersed Solids," Journal of Engineering for Industry, ASME, Vol. 94, pp. 167-173, 1977.

3. Liu, W. K., Lam, D. and Belytschko, T., "Finite Element Method for Hydrodynamic Mass with Nonstationary Fluid," Computer Methods in Applied Mechanics and Engineering, Vol. 44, pp. 177-211, 1984.

4. Liu, W. K. and Ma, D., "Computer Implementation Aspects for Fluid Structure Interaction Problems," Computer Methods in Applied Mechanics and Engineering, Vol. 31, pp. 129-148, 1982.

5. Liu, W. K. and Chang, H. G., "Efficient Computational Procedures for Long-Time Duration Fluid-Structure Interaction Problems," Journal of Pressure Vessel Technology, ASME, Vol. 106, pp. 317-322, 1984.

6. Hughes, T. J. R., Liu, W. K. and Zimmerman, T. K., "Lagrangian-Eulerian Finite Element Formulation for Incompressible Viscous Flows," Computer Methods in Applied Mechanics and Engineering, Vol. 29, pp. 329-349, 1981.

7. Liu, W. K., Belytschko, T. and Chang, H., "An Arbitrary Lagrangian-Eulerian Finite Element Method for Path-Dependent Materials," Computer Methods in Applied Mechanics and Engineering, Vol. 58, pp. 227-246, 1986.

8. Brooks, A. N. and Hughes, T. J. R., "Streamline Upwind/Petrov-Galerkin Formulations for Convection Dominated Flows with Particular Emphasis on the Incompressible Navier-Stokes Equations," Computer Methods in Applied Mechanics and Engineering, Vol. 32, pp. 199-259, 1982.

9. Hughes, T. J. R. and Brooks, A. N., "A Theoretical Framework for Petrov-Galerkin Methods with Discontinuous Weighting Functions: Application to the Streamline-Upwind Procedure," in Finite Elements in Fluids, Vol. 4, Gallagher, R. H., Norrie, D. H., Oden, J. T. and Zienkiewicz, O. C., eds., John Wiley and Sons, Ltd., pp. 47-65, 1982.

10. Liu, W. K. and Chang, H. G., "A Method of Computation for Fluid Structure Interaction," Journal of Computers and Structures, Vol. 20, No. 1-3, pp. 311-320, 1985.

11. Pattani, P. G. and Olson, M. D., "Periodic Solutions of Rigid Body-Viscous Flow Interaction," preprint.

12. Hughes, T. J. R. and Tezduyar, T. E., "Finite Element Methods for First-Order Hyperbolic Systems with Particular Emphasis on the Compressible Euler Equations," Computer Methods in Applied Mechanics and Engineering, Vol. 45, pp. 217-284, 1984.

Figure Captions

Figure 1. Problem Statement.

Figure 2. Mesh discretization a) Complete Domain, b) Imposed Mesh Distortion.

Figure 3. Instantaneous Streamlines for $\beta = 0.1$ and $R_w = 20$ at a) $t = 0$, b) $t = \frac{\pi}{4}$, c) $t = \frac{\pi}{2}$, d) $t = \frac{3\pi}{4}$.

Figure 4. Instantaneous Streamlines for $\beta = 0.1$ and $R_w = 500$ at a) $t = 0$, b) $t = \frac{\pi}{4}$, c) $t = \frac{\pi}{2}$, d) $t = \frac{3\pi}{4}$.

Figure 5. Vortex Formation for $\beta = 1.0$ and $R_w = 1000$ at a) $t = \frac{\pi}{2}$, b) $t = \frac{3\pi}{4}$.

Figure 6. Pressure Distribution around the solid for $\beta = 0.1$ and a) $R_w = 20$, b) $R_w = 500$.

Figure 7. Fluid Force versus Time for the Decomposition of F_f in Mass and Damping terms with $\beta = 0.1$.

Figure 8. Dimensionless Mass ($\overline{M}_{ad}$) versus Frequency Reynolds Number (R_w).

Figure 9. Dimensionless Damping ($\overline{C}_{ad}$) versus Frequency Reynolds Number (R_w).

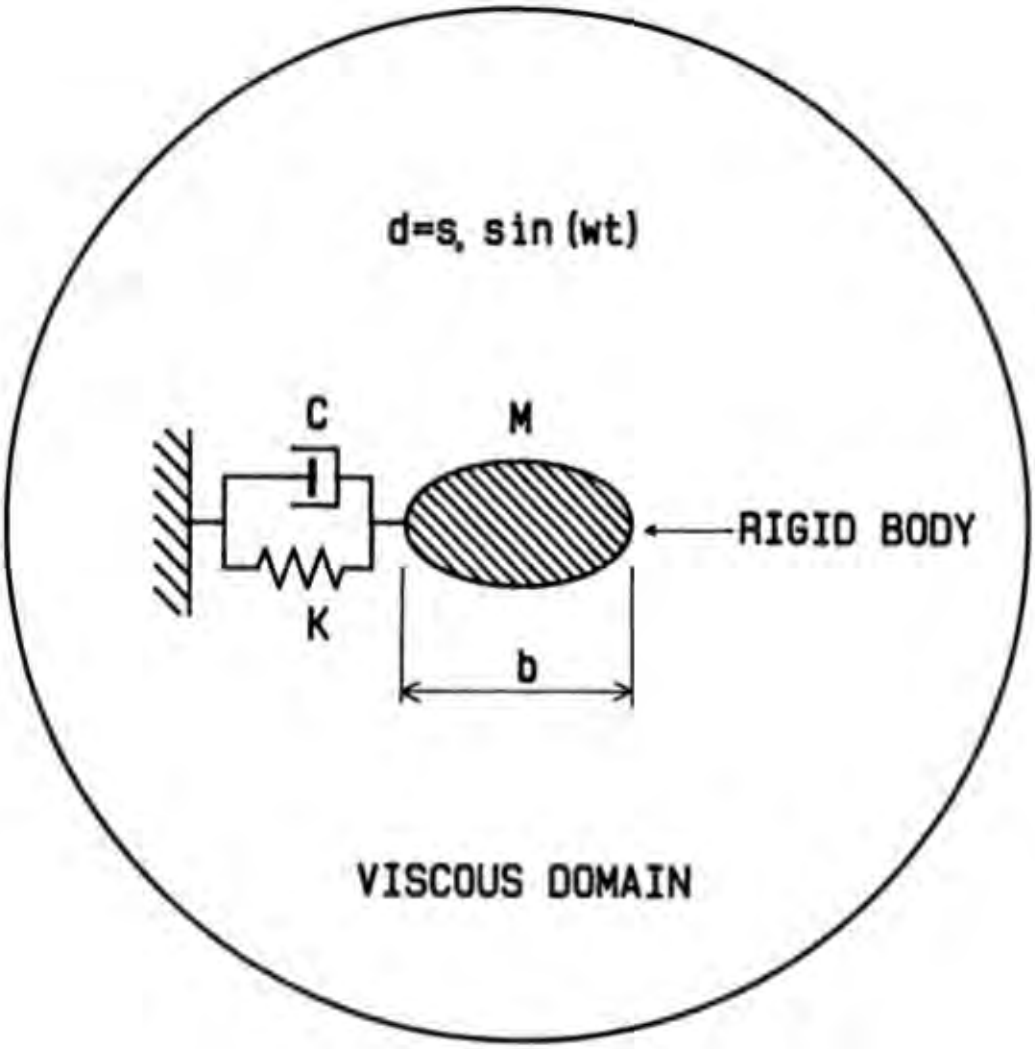

Fig 1

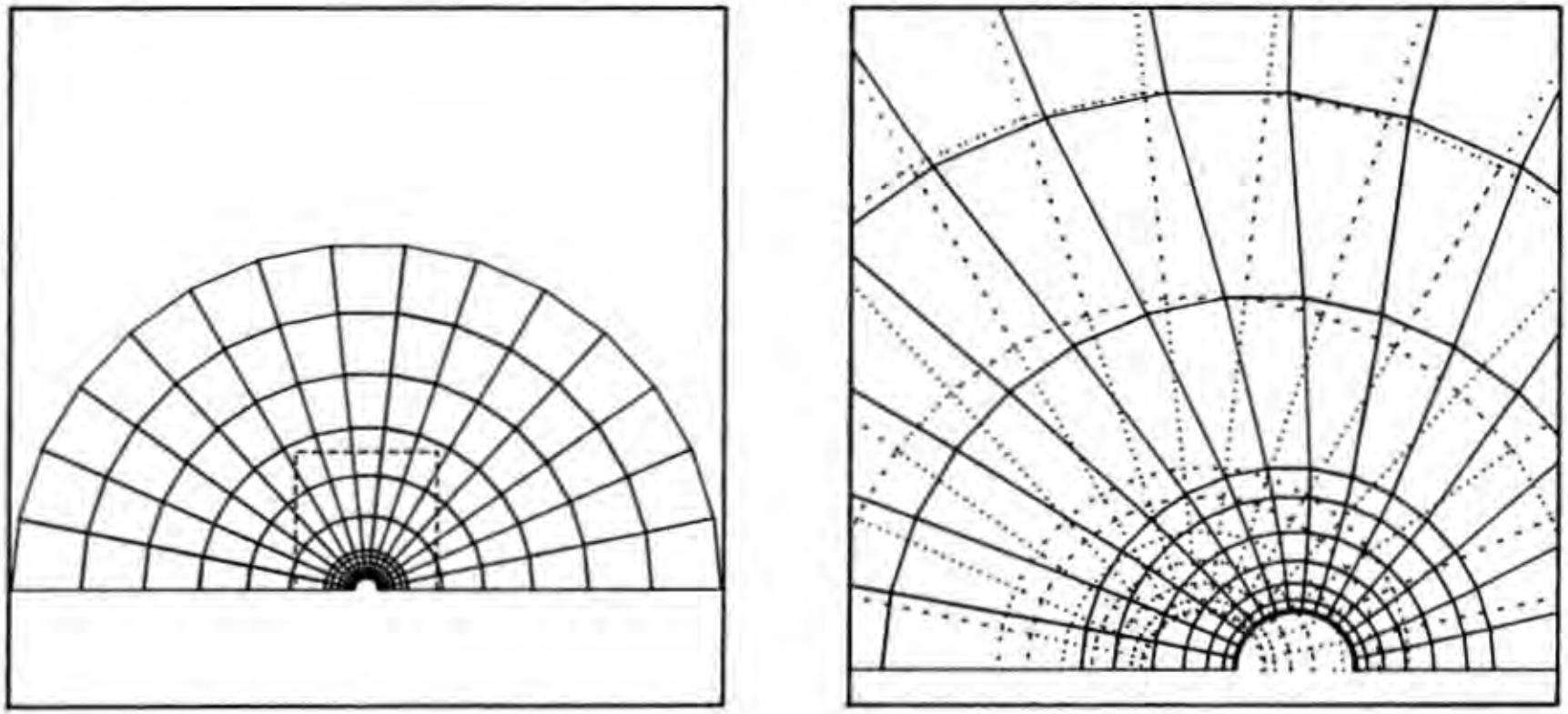

Fig 2

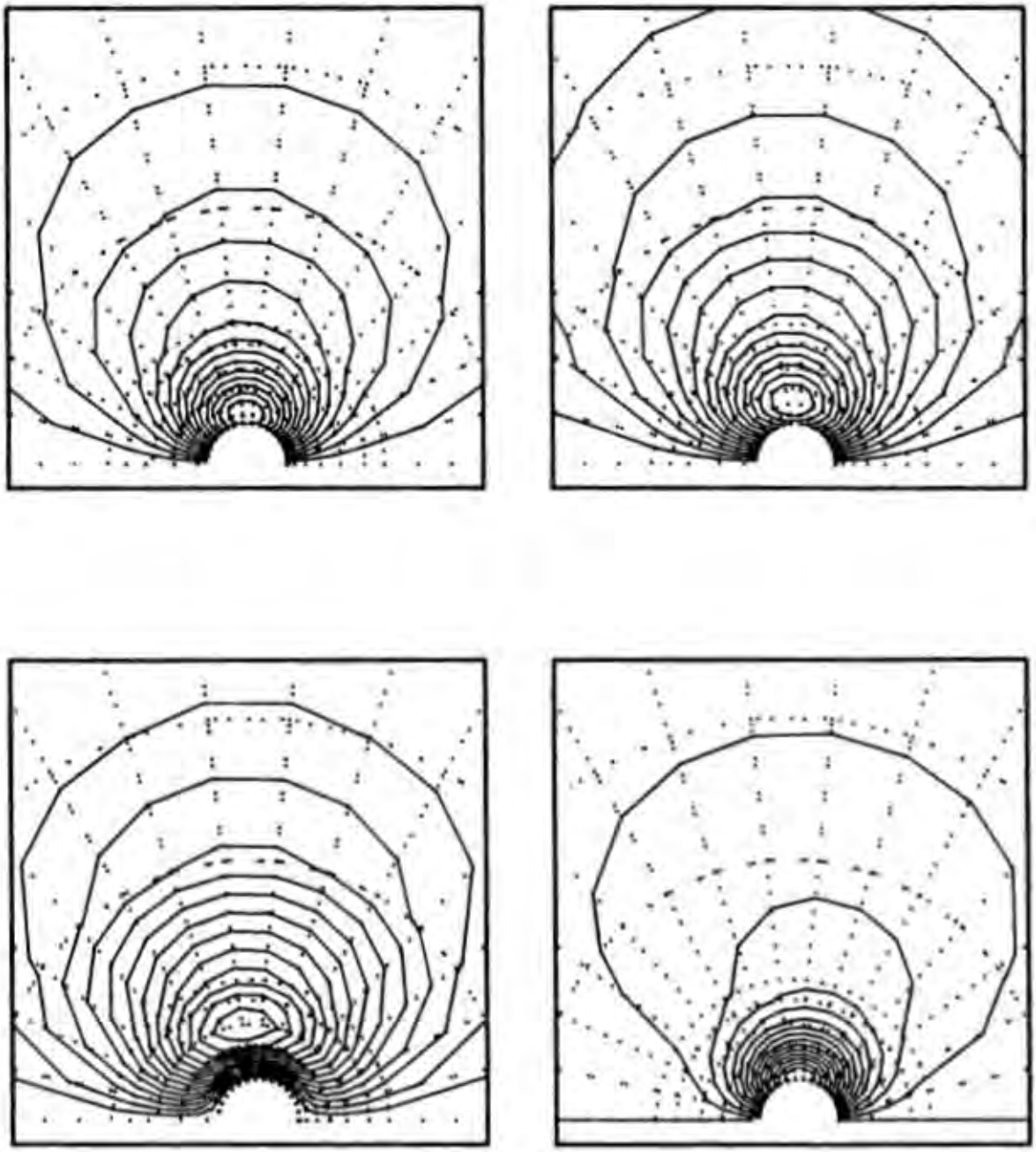

Fig 3

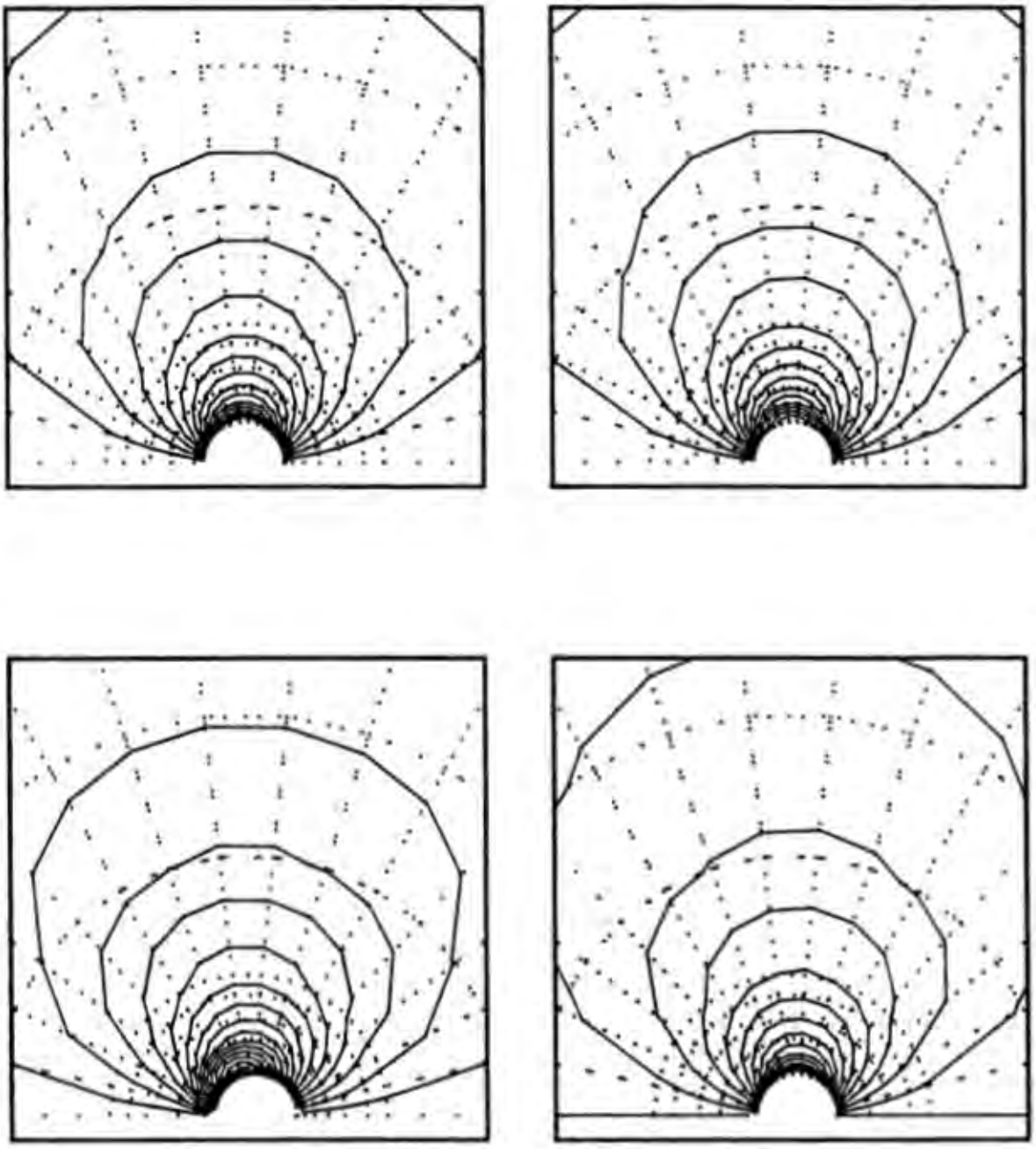

Fig 4

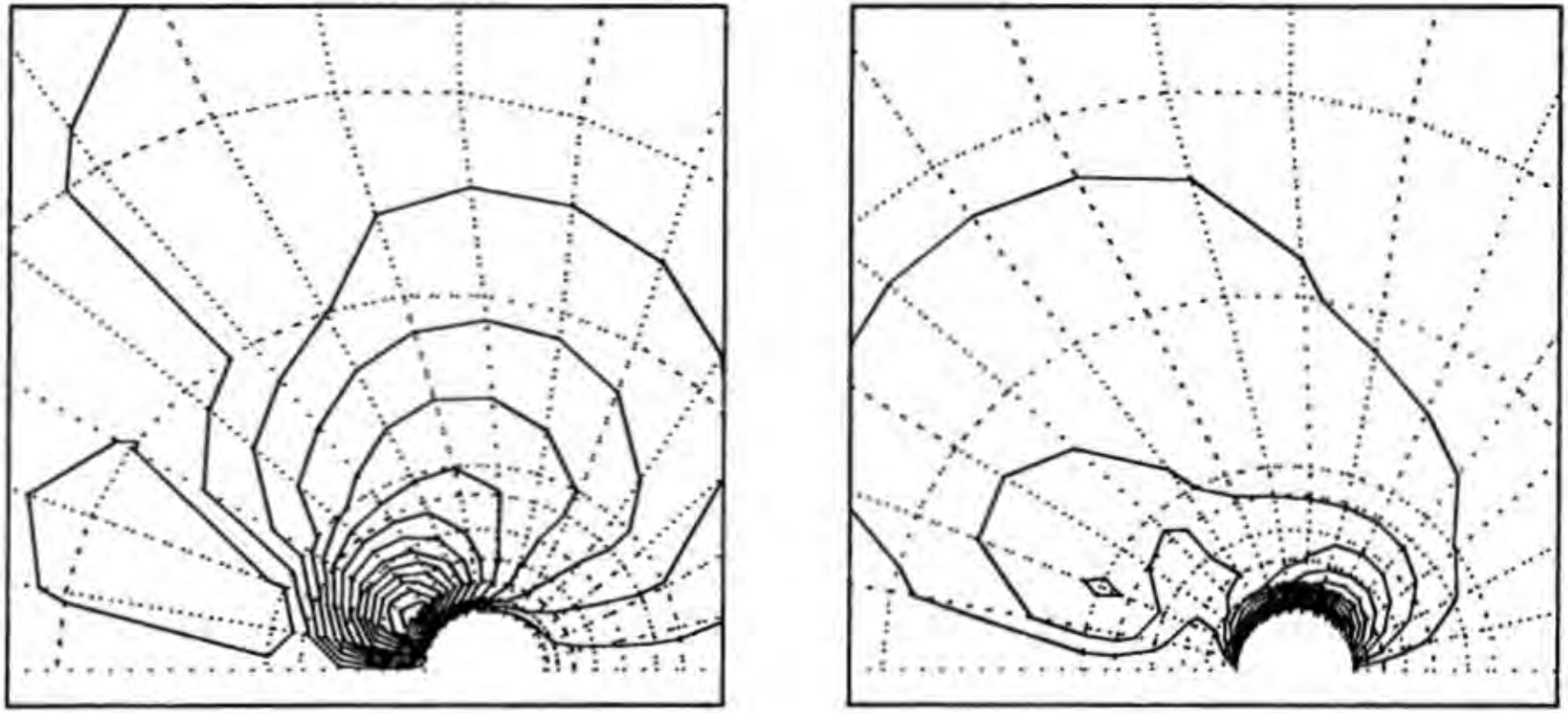

Fig 5

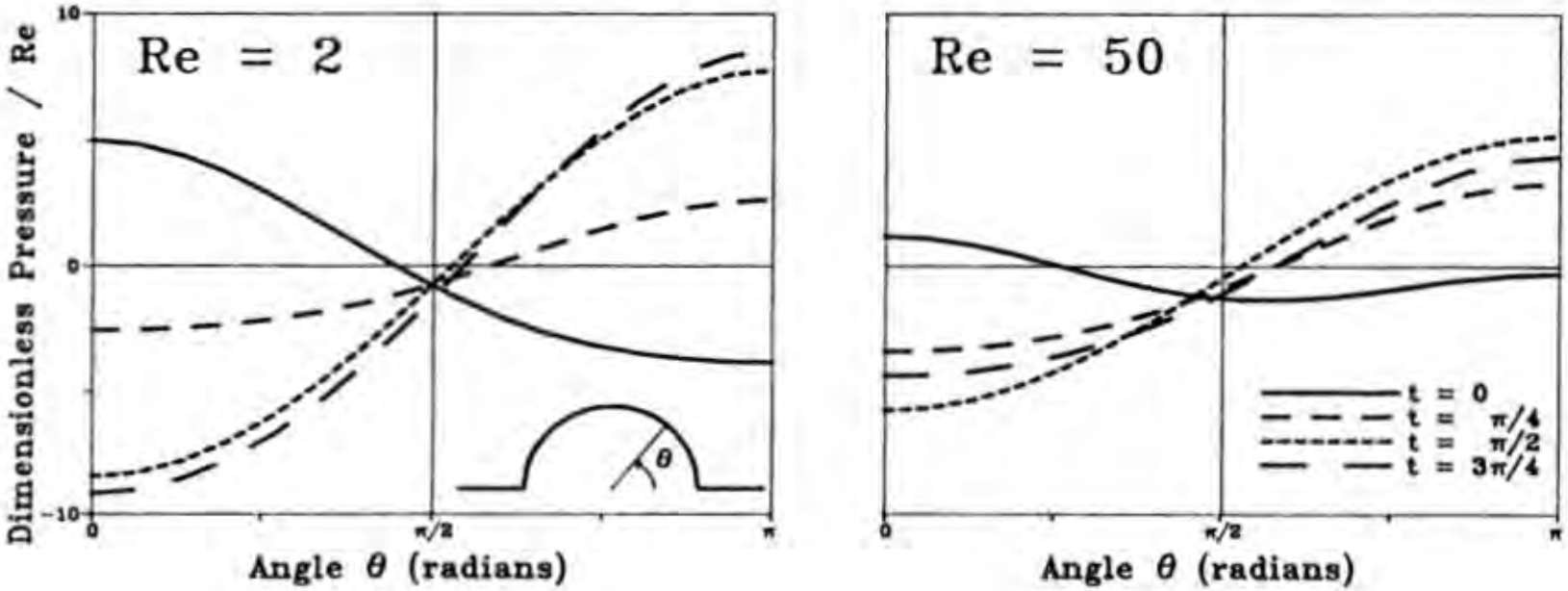
Re = 2
Re = 50
Dimensionless Pressure / Re
10
0
-10
0
π/2
π
θ
Angle θ (radians)
t = 0
t = π/4
t = π/2
t = 3π/4

Fig 6

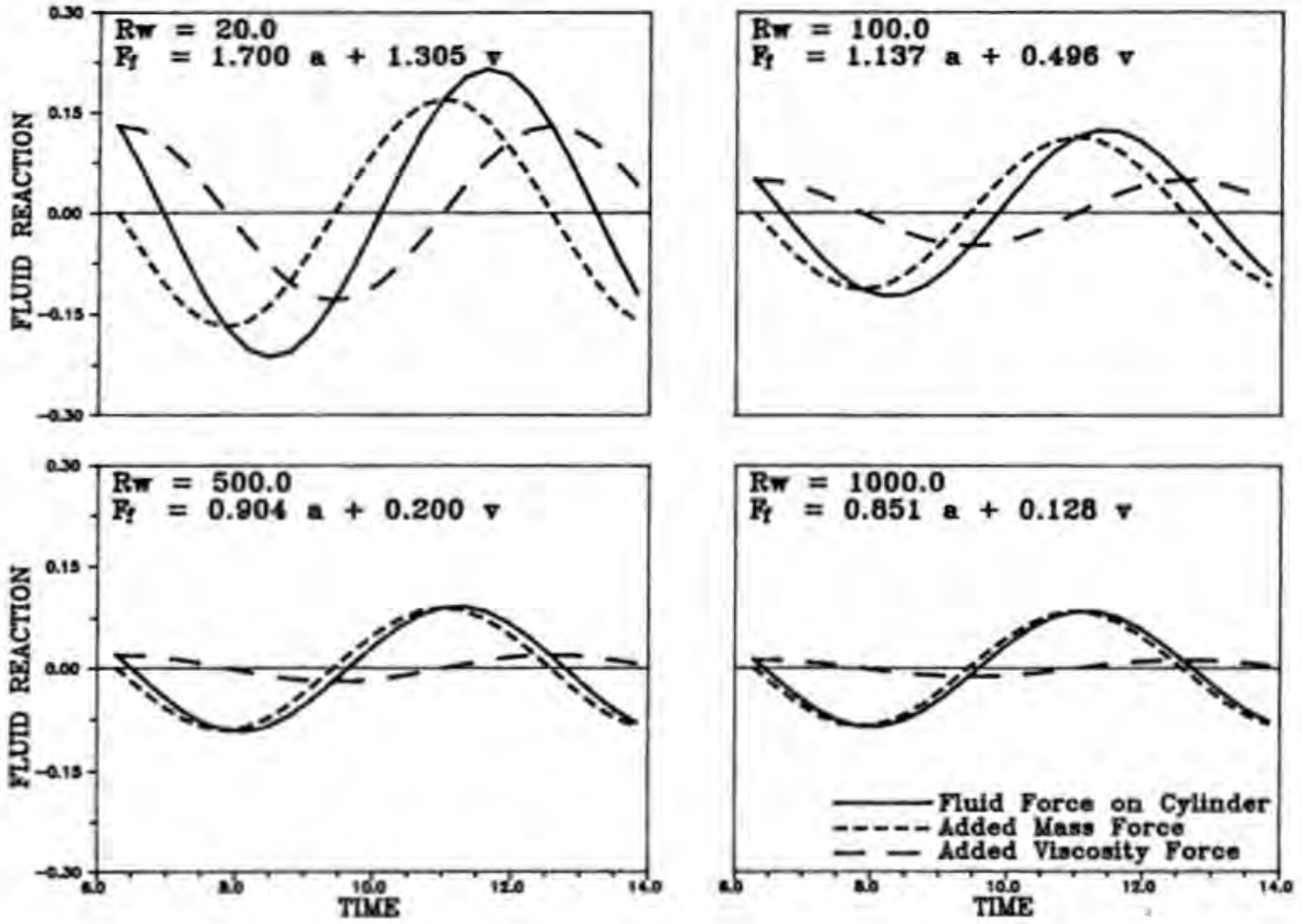
Rw = 20.0
Ff = 1.700 a + 1.305 v
Rw = 100.0
Ff = 1.137 a + 0.496 v
Rw = 500.0
Ff = 0.904 a + 0.200 v
Rw = 1000.0
Ff = 0.851 a + 0.128 v
FLUID REACTION
TIME
Fluid Force on Cylinder
Added Mass Force
Added Viscosity Force

Fig. 7

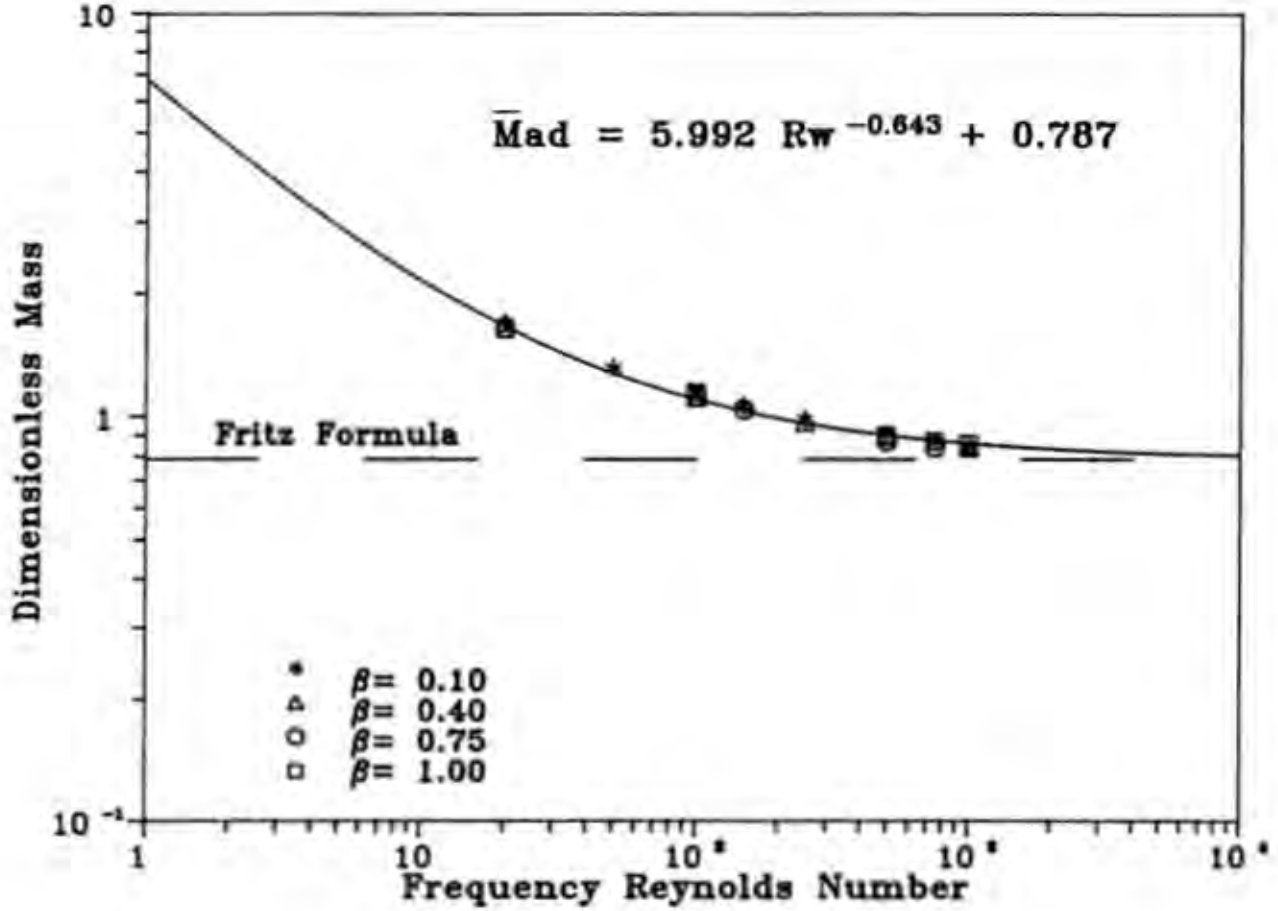
10
1
10^{-1}
$\bar{M}ad = 5.992\ Rw^{-0.643} + 0.787$
Fritz Formula
β= 0.10
β= 0.40
β= 0.75
β= 1.00
Dimensionless Mass
1
10
10^{2}
10^{3}
10^{4}
Frequency Reynolds Number

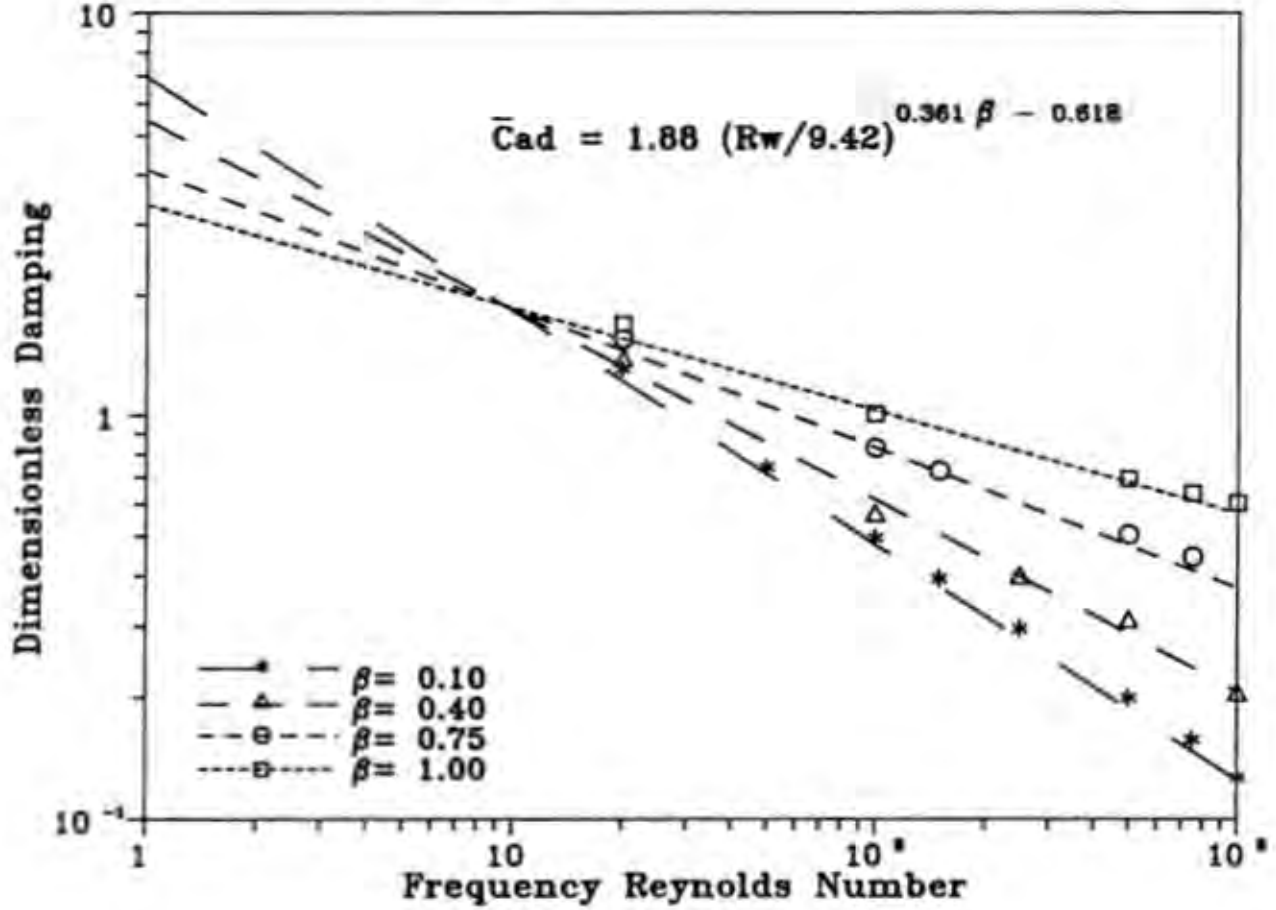
10
1
10^{-1}
$\bar{C}ad = 1.88\ (Rw/9.42)^{0.361\,\beta\ -\ 0.618}$
Dimensionless Damping
β= 0.10
β= 0.40
β= 0.75
β= 1.00
1
10
10^{2}
10^{3}
Frequency Reynolds Number

Fig 9